GEOLOGICA CARPATHICA, OCTOBER 2018, 69, 5, 453–466 doi: 10.1515/geoca-2018-0026

Petrology and dating of the Permian lamprophyres from the Malá Fatra Mts. (Western Carpathians, Slovakia)

JÁN SPIŠIAK[1], LUCIA VETRÁKOVÁ[1], DAVID CHEW[2], ŠTEFAN FERENC[1], TOMÁŠ MIKUŠ[3], VIERA ŠIMONOVÁ[1] and PETER BAČÍK[3,4]

[1]Faculty of Natural Sciences, Matej Bel University, Tajovského 40, 974 01 Banská Bystrica, Slovakia; jan.spisiak@umb.sk
[2]Department of Geology, Trinity College Dublin, Dublin 2, Ireland
[3]Earth Science Institute, Slovak Academy of Sciences, Dúbravská cesta 9, 840 05 Bratislava, Slovakia
[4]Department of Mineralogy and Petrology, Faculty of Natural Sciences, Comenius University in Bratislava, Ilkovičova 6, 842 15 Bratislava, Slovakia

(Manuscript received November 3, 2017; accepted in revised form October 4, 2018)

Abstract: Calc–alkaline lamprophyres are known from several localities in the Malá Fatra Mountains. They form dykes (0.5–3 m) of varying degree of alteration that have intruded the surrounding granitoid rocks which are often incorporated xenoliths. Clinopyroxenes (diopside to augite), amphiboles (kaersutitic), biotites (annite) and plagioclases are major primary minerals of the dykes, accessory minerals include apatite, ilmenite, rutile, pyrite, chalcopyrite, and pyrrhotite. Apatite has a relatively low F, but increased Cl content compared to typical apatite from lamprophyres or magmatic apatite from granitic rocks in the Western Carpathians. The chemical composition of the lamprophyres indicates their calc–alkaline character, but affinity to alkaline lamprophyres is suggested by the Ti enrichment in clinopyroxene, amphibole and biotite. According to modal classification of the minerals, the studied rocks correspond to spessartite. The differences in the chemical composition of the rocks (including Sr and Nd isotopes) probably result from the contamination of primary magma by crustal material during magma ascent. The age of the lamprophyres, based on U/Pb dating in apatite, is 263.4±2.6 Ma.

Keywords: calc–alkaline lamprophyres, mineralogy, geochemistry, Malá Fatra Mts.

Introduction

Lamprophyres are dyke rocks which differ from intrusive and effusive rocks in mineral composition, structure and, to some degree, chemical composition. The term lamprophyre was introduced by Gümbel (1874) to denote dark-coloured dyke rocks of variable mineral composition.

Lamprophyres are generally ultramafic, mafic, or intermediate rocks that intrude the basement at shallow-crustal levels and form dykes or sills. They are porphyritic rocks comprising phenocrysts of mafic minerals in a groundmass consisting of the same early crystallized minerals. The early magmatic mafic minerals include phlogopite, olivine, amphibole, clinopyroxene, and apatite (Bergman 1987; Rock 1987, 1991). The lamprophyric magmas are typically formed at low degrees of partial melting of an upper mantle source at a depth of 100–150 km (Rock 1991). These magmas are known to have very high concentrations of volatiles (F, CO_2, H_2O) and incompatible trace elements (light REE, Zr, Sr, Ba). Such high volatile contents likely result either from a previously volatile and incompatible elements-rich mantle source (Ulrych et al. 1993) or from fluid-rich metasomatism (McKenzie 1989). Lamprophyres cannot be simply referred to as textural varieties of common plutonic or volcanic rocks, they are more complex in nature (Seifert 2005). They are hybrid rocks, resulting from interactions of mantle melts with more evolved crustal material by processes of magma mixing (mafic–felsic melts) and/or assimilation of country-rock material (Rock 1991).

In the crystalline complexes of the Western Carpathians, lamprophyres occur in various core mountains: Považský Inovec Mts., Suchý Mts., Malá Fatra Mts., Nízke Tatry Mts., but they are also known from the Veporic complexes (Hovorka 1967). Yet no attention has been paid to the detailed mineralogical and geochemical characteristics and age of these rocks. The focus of this work is on the detailed study of the mineral composition and geochemistry of Malá Fatra Mts. lamprophyres.

Geological setting

Basic dyke rocks from the Malá Fatra Mts. were first described by Ivanov and Kamenický (1957) from the area of the Kriváň hill (elevation Veľká Kráľová) and Martinské hole Mountains. The rocks occur as dykes of different thickness (0.5–3 m). Hovorka (1967) labelled these rocks as monsonitic lamprophyres. Lamprophyres are found in the surroundings of granitoid rocks (granodiorite and tonalite) of the Western Carpathians crystalline complexes. Some of the Malá Fatra lamprophyre dykes were relatively strongly tectonically affected, which indicates their pre-Alpine age. Depending on the structure, texture and mineral composition of

lamprophyres, several types of dyke rocks can be distinguished in the Malá Fatra Mts.: porphyric, equigranular and amygdaloidal. Lamprophyres were studied from two localities (Fig. 1):

- Outcrops of dykes at the cable car valley station at Martinské hole near Kalužná hill (49°5'49" N, 18°50'28" E).
- Dykes in Dubná skala granite quarry (49°8'25" N, 18°52'43" E) and dykes from the Višňové highway tunnel gallery.

The studied lamprophyres often contain xenoliths of the surrounding granitoid rocks and their minerals resorbed in a different stage. The surrounding granitoid rocks have the character of hybrid tonalities (Kamenický et al. 1987) or I-type granites (Broska et al. 1997). The minerals represented in the rocks are mainly plagioclases (oligoclase–andesine), strongly undulosed quartz, less potassium feldspar and biotites, and relatively rarely muscovite.

Mesozoic sequences of the Malá Fatra also contained Cretaceous alkaline lamprophyres (Polom, Višňové or Krpeľany; Hovorka & Spišiak 1988; Spišiak 1999). They are different in age, mineral and chemical composition, but above all, in the presence of foids and absence of quartz and feldspar.

Analytical methods

Silicates and apatites were studied using electron microprobe JEOL JXA 8530FE at the Earth Sciences Institute of the Slovak Academy of Sciences in Banská Bystrica under the following conditions for silicates: accelerating voltage 15 kV, probe current 20 nA, beam diameter 3–8 μm, ZAF correction, counting time 10 s on peak, 5 s on background. The used standards, X-ray lines and D.L. (in ppm) were: Ca(*Kα*, 25) — diopside; K (*Kα*, 44) — orthoclase; P (*Kα*, 41) — apatite; F (*Kα*, 167) — fluorite; Na (*Kα*, 43) — albite; Mg (*Kα*, 41) — diopside; Al (*Kα*, 42) — albite; Si (*Kα*, 63) — quartz; Ba (*Lα*, 72) — barite; Fe (*Kα*, 52) — hematite; Cr (*Kα*, 113) — Cr_2O_3; Mn (*Kα*, 59) — rhodonite; Ti (*Kα*, 130) — rutile; Cl (*Kα*, 12) — tugtupite; Sr (*Lα*, 71) — celestite. The following conditions for apatites were used: accelerating voltage 15 kV, probe current 20nA and beam diameter 5 μm and ZAF matrix correction was used. The EPMA was calibrated by the natural and synthetic standards. Used standards, X-ray lines, crystal and D.L. (in ppm) are: Ca (*Kα*, PETL, 24–62) — diopside; K (*Kα*, PETL, 20–48) — orthoclase; Th (*Mα*, PETL, 41–75) — thorianite; Pb (*Mβ*, PETL, 65–138) — crocoite; Cl (*Kα*, PETL, 11–12) — tugtupite; P (*Kα*, PETL, 56–85) — apatite; S (*Kα*, PETL, 27–47) — barite; Y — (*Lα*, PETL, 59–122) — YPO_4; F (*Kα*, LDE1, 103–273) — fluorite; Na (*Kα*, TAP, 46–78) — albite; Sr (*Lα*, TAP, 38–201) — celestite; Si (*Kα*, TAP, 50–125) — orthoclase; Al (*Kα*, TAP, 37–100) — albite; Mg (*Kα*, TAP, 37–87) — diopside; Sm (*Lβ*, LIFH, 62–274) — $SmPO_4$; Pr (*Lβ*, LIFH, 121–235) — $PrPO_4$; Nd (*Lα*, LIFH, 62–123) — $NdPO_4$; Ce (*Lα*, LIFH, 65–129) — $CePO_4$; La (*Lα*, LIFH, 72–139) — $LaPO_4$; Fe (*Kα*, LIF, 94–333) — hematite; Mn (*Kα*, LIF, 79–238) — rhodonite; Ti (*Kα*, LIF, 133–333) — rutile; Ba (*Lα*, LIF, 242–674) — barite.

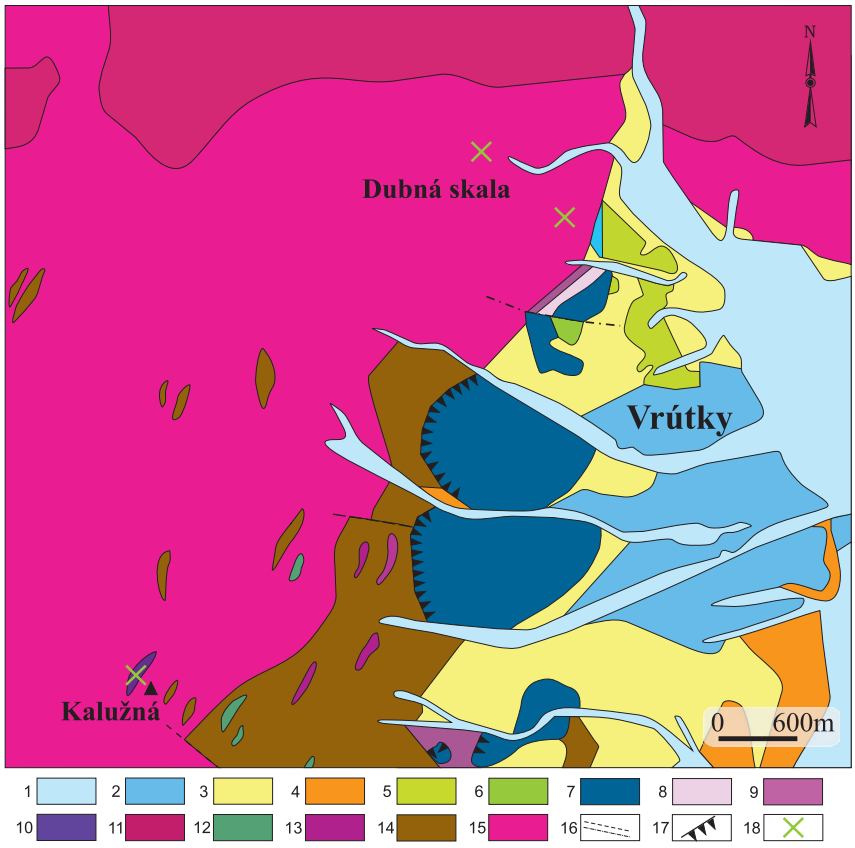

Fig. 1. Geological map of part of Malá Fatra Mts. (Digital geological map of the Slovak Republic at scale 1:50,000 [online]. State Geological Institute of Dionýz Štúr, Bratislava, 2013). Legend: 1 — fluvial sediments (Quaternary); 2 — proluvial sediments (Quaternary); 3 — deluvial sediments (Quaternary); 4 — Martin Fm. (calcareous clays, sandstones, conglomerates, Quaternary); 5 — Dubná Skala Fm. (nonsaline limestones, travertines, alms, conglomerates, Miocene); 6 — Mráznica Fm. (grey and dark-gray marly limestones, alms, marlestones, Late Jurassic–Early Cretaceous); 7 — Allgäu Fm. (Early Jurassic); 8 — Guttenstein Limestones (Middle Triassic); 9 — Lúžna Fm. (Early Triassic); 10 — porfyrites, porphyrites, lamprophyres (Late Paleozoic); 11 — granites and granodiorites (Early Paleozoic); 12 — amphibolites (Early Paleozoic); 13 — orthogneisses (Early Paleozoic); 14 — garnet–biotite paragneisses (Early Paleozoic); 15 — granodiorites and tonalities (Early Paleozoic); 16 — fault lines; 17 — tectonic structure (nappe structure); 18 — samples.

The chemical composition of the rocks was determined at the ACME Analytical Laboratories (Vancouver, Canada). Total abundances of major element oxides were determined by inductively coupled plasma–emission spectrometry (ICP-ES) following lithium metaborate–tetraborate fusion and dilute nitric acid treatment. Loss on ignition (LOI) was calculated from the difference in weight after ignition to 1000 °C. For the total carbon (TOT/C) and sulphur analysis (TOT/S) by LECO analysis, the samples were heated in an induction furnace to >1650 °C, which caused volatilization of all C and S bearing phases. Vapours were carried through an infrared spectrometric cell wherein the concentrations of C and S were determined by the absorption of specific wavelengths in the infrared spectra (ORG/C=TOT/C minus graphite C and carbonate). Concentrations of trace elements and rare earth elements were determined by ICP mass spectrometry (ICP-MS). Further details are accessible on the web page of the ACME Analytical Laboratories (http://acmelab.com/).

Apatite crystals were separated using standard techniques. Apatite U–Pb data were acquired using a Photon Machines Analyte Exite 193 nm ArF Excimer laser-ablation system coupled to a Thermo Scientific iCAP Qc at the Department of Geology Trinity College Dublin. Twenty-eight isotopes (^{31}P, ^{35}Cl, ^{43}Ca, ^{55}Mn, ^{86}Sr, ^{89}Y, ^{139}La, ^{140}Ce, ^{141}Pr, ^{146}Nd, ^{147}Sm, ^{153}Eu, ^{157}Gd, ^{159}Tb, ^{163}Dy, ^{165}Ho, ^{166}Er, ^{169}Tm, ^{172}Yb, ^{175}Lu, ^{200}Hg, ^{204}Pb, ^{206}Pb, ^{207}Pb, ^{208}Pb, ^{232}Th, ^{238}U and mass ^{248}(^{232}Th^{16}O) were acquired using a 50 μm laser spot, a 4 Hz laser repetition rate and a fluence of 3.31 J/cm^2. A ca. 1 cm sized crystal of Madagascar apatite which has yielded a weighted average ID-TIMS concordia age of 473.5±0.7 Ma (Thomson et al. 2012; Cochrane et al. 2014) was used as the primary apatite reference material in this study. McClure Mountain syenite apatite (the rock from which the ^{40}Ar/^{39}Ar hornblende standard MMhb is derived) was used as a secondary standard. McClure Mountain syenite has moderate but reasonably consistent U and Th contents (~23 ppm and 71 ppm; Chew & Donelick 2012) and its thermal history, crystallization age (weighted mean ^{207}Pb/^{235}U age of 523.51±2.09 Ma) and initial Pb isotopic composition (^{206}Pb/^{204}Pb=17.54±0.24; ^{207}Pb/^{204}Pb=15.47 ±0.04) are known from high-precision TIMS analyses (Schoene & Bowring 2006). Durango apatite was also analysed in this study as a secondary standard. Durango apatite is a distinctive yellow-green fluorapatite widely used as a mineral standard in apatite fission-track and (U–Th)/He dating and apatite electron micro-probe analyses. It is found as large crystals within an open pit iron mine at Cerro de Mercado, Durango, Mexico. The apatite was formed between the eruptions of two major ignimbrites which have yielded a sanidine–anorthoclase ^{40}Ar–^{39}Ar age of 31.44±0.18 Ma (McDowell et al. 2005). NIST 612 standard glass was used as the apatite trace element concentration reference material. The raw isotope data were reduced using the "VizualAge" data reduction scheme of Petrus & Kamber (2012) within the freeware IOLITE package of Paton et al. (2011). User-defined time intervals are established for the baseline correction procedure to calculate session-wide baseline-corrected values for each isotope. The time-resolved fractionation response of individual standard analyses is then characterized using a user-specified down-hole correction model (such as an exponential curve, a linear fit or a smoothed cubic spline). The data reduction scheme then fits this appropriate sessionwide "model" U–Th–Pb fractionation curve to the time-resolved standard data and the unknowns. Sample-standard bracketing is applied after the correction of down-hole fractionation to account for long-term drift in isotopic or elemental ratios by normalizing all ratios to those of the U–Pb reference standards. Common Pb in the apatite standards was corrected using the ^{207}Pb-based correction method using a modified version of the VizualAge DRS that accounts for the presence of variable common Pb in the primary standard materials (Chew et al. 2014). Over the course of two months of analyses, McClure Mountain apatite (^{207}Pb/^{235}U TIMS age of 523.51±1.47 Ma; Schoene & Bowring 2006) yielded a U–Pb Tera-Wasserburg concordia lower intercept age of 524.5±3.7 Ma with an MSWD=0.72. The lower intercept was anchored using a ^{207}Pb/^{206}Pb value of value of 0.88198 derived from an apatite ID-TIMS total U–Pb isochron (Schoene & Bowring 2006).

Samples for Sr and Nd isotope analyses were chemically prepared and measured in the Isotope Geochemistry Laboratory in the Institute of Geological Sciences of the Polish Academy of Science, Krakow. The analyses were made with a Multi-Collector Inductively Coupled Plasma Mass Spectrometer (MC-ICP-MS) Neptune. The samples were digested in three steps: firstly, with HF : HNO_3, secondly, with HNO_3 and finally, with HCl and HF, following the procedure described by Anczkiewicz et al. (2004) and Anczkiewicz & Thirlwall (2003). The samples were then dissolved in HCl for loading on cation exchange columns with AG50Wx8 resin (Anczkiewicz et al. 2004). Final separation of Sr was performed by Sr-spec resin (Peryt et al. 2010) and Nd by Ln-spec resin (Anczkiewicz & Thirlwall 2003). Nd isotopes were normalized to ^{143}Nd/^{144}Nd=0.7219 to correct for mass bias. The reproducibility of Nd standards over the period of analyses was ^{143}Nd/^{144}Nd=0.512101±8 (2 s.d. n=3). Sr isotopes were normalized to ^{86}Sr/^{88}Sr=0.1194 to correct for mass bias. The reproducibility of Sr standards over the period of analyses was ^{87}Sr/^{86}Sr=0.710261±8 (2 s.d. n=3). They were also chemically prepared and measured in the Isotope Geochemistry Laboratory in the Institute of Geological Sciences of the Polish Academy of Science, Krakow. The εNd(0,t) values were calculated with parameters for CHUR ^{143}Nd/^{144}Nd=0.512638, ^{147}Sm/^{144}Nd=0.1967 (Jacobsen & Wasserburg 1980; DePaolo 1981).

Results

Petrographic observation

Lamprophyres from the Malá Fatra Mountains are pale green, grey-green to dark grey in colour and they mostly have porphyric texture (equigranular types are less frequent), rarely

also amygdaloidal texture. Phenocrysts are formed by plagioclase, quartz, pyroxene, biotite, rarely also amphibole. In some places, there are occurrences of irregular, up to 6 cm large xenoliths of the surrounding granitoid rocks or their minerals (mainly plagioclases; Fig. 2a). Oval-shaped amygdales filled with carbonate, rarely with chlorite are also frequent (Fig. 2b). The rocks are characterized by strongly, usually almost completely altered primary minerals, namely clinopyroxenes, but often also amphiboles and biotites. This is the reason for difficulties in the classification of rocks based on their modal mineral composition composition (Spišiak & Hovorka 1998). Nevertheless, based on the observed relics of minerals, their pseudomorphoses and types of alterations, the studied rocks correspond to spessartite. The chemical and isotopic compositions of the lamprophyres from the Malá Fatra Mts. in the analysed samples are given in Tables 1 and 2.

We determined the age of the rocks using LA-ICP-MS by apatite analysis (Trinity College, Dublin, Ireland) as 263.4±2.6 Ma (Fig. 3), which corresponds well to their geological position.

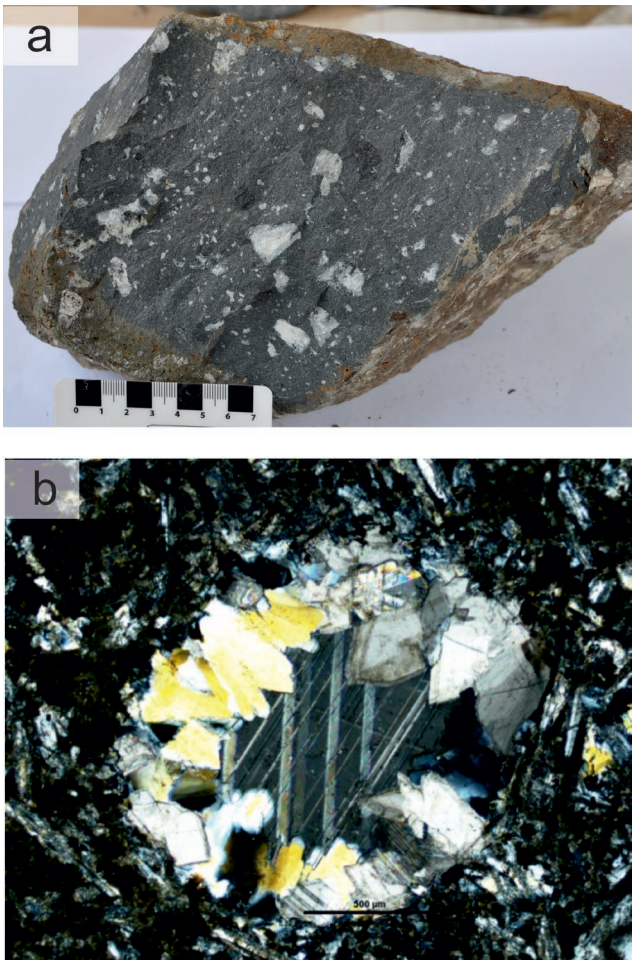

Fig. 2. a — Photo of the lamprophyres structure; light irregular shape — xenolith of the surrounded granitoids, small ovoid-shape carbonate amygdaloids; **b** — photomicrograph of carbonate amygdales, crossed polaroids.

Mineralogical characterization

Clinopyroxenes usually form phenocrysts with a typical oscillatory and sector (hour-glass texture) (Fig. 4a) zoning. The pyramidal sector is enriched with SiO_2 and MgO, or depleted in TiO_2, Al_2O_3 and Na_2O compared to the prismatic sector (Table 3). The studied clinopyroxenes are characterized by relatively high contents of TiO_2 and Na_2O. Based on the IMA classification of pyroxenes (Morimoto et al. 1988), they

Table 1: Chemical composition of lamprophyres from the Malá Fatra Mts.

	MH-1	MH-2	DS-55	DS-424
SiO_2	39.96	46.85	53.22	48.10
TiO_2	1.65	1.85	1.63	1.75
Al_2O_3	14.05	16.64	15.68	15.92
Fe_2O_3	9.88	10.68	8.44	9.97
Cr_2O_3	0.02	0.02	0.02	0.03
MnO	0.16	0.18	0.08	0.16
MgO	6.55	5.38	7.23	6.88
CaO	9.40	4.76	1.77	6.36
Na_2O	3.24	3.20	4.39	2.95
K_2O	1.82	3.59	1.34	1.63
P_2O_5	0.60	0.66	0.46	0.44
LOI	12.30	5.80	5.50	5.50
Total	99.63	99.73	99.76	99.73
TOT/C	2.91	0.83	0.27	0.51
TOT/S	0.08	0.07	0.07	0.06
Sc	14	15	17	18
Ba	433	1052	308	425
Be	2	2	2	1
Co	27.8	27.9	18.6	33.7
Cs	1.5	1.7	1.4	1.6
Ga	13.6	16.1	15.6	15.6
Hf	4.9	5.5	5.4	5.1
Nb	53.8	66.2	53.1	47.3
Rb	41.1	60.3	20.5	36.7
Sn	2	2	2	2
Sr	571.7	589.4	113.9	509.3
Ta	3.4	4.1	3.4	3.0
Th	4.5	5.7	5.8	5.9
U	21	2	2.3	2
V	117	128	139	158
W	0.7	0.5	1.3	1
Zr	219	273.5	241.4	220.9
Y	21.3	25.7	22.8	24.5
La	39.9	50.1	33.7	37.7
Ce	79.6	87.7	69.2	73
Pr	8.69	10.04	7.71	8.17
Nd	32.2	36.8	28.2	31.3
Sm	5.45	6.37	5.28	6.14
Eu	1.83	1.97	1.59	1.7
Gd	5.18	5.73	5.2	5.47
Tb	0.74	0.84	0.7	0.8
Dy	4.3	4.6	4.17	4.64
Ho	0.77	0.95	0.79	0.9
Er	2.16	2.67	2.28	2.49
Tm	0.32	0.38	0.34	0.37
Yb	1.98	2.48	2.24	2.24
Lu	0.32	0.35	0.37	0.37
Ni	52	52	73	80

Table 2: Sr and Nd isotope composition of studied lamprophyres.

	Age	$^{143}Nd/^{144}Nd$	2SE	$^{143}Nd/^{144}Ndi$	EpsNdi	$^{87}Sr/^{86}Sr$	2SE	$^{87}Sr/^{86}Sri$
DS-424	260	0.512725	0.000006	0.512523	4.29	0.705136	0.000008	0.704365
DS-55	260	0.5127624	0.000009	0.5127	5.2	0.707219	0.000011	0.705292
MH-1	260	0.512817	0.000005	0.512643	6.63	0.704381	0.000007	0.703612
MH-2	260	0.512813	0.000006	0.512635	6.47	0.704406	0.000008	0.703311

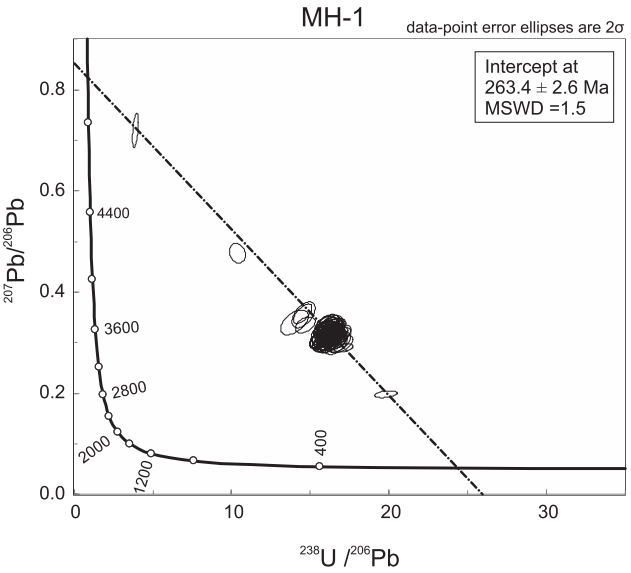

Fig. 3. LA-ICP-MS U–Pb age for apatite from studied lamprophyres.

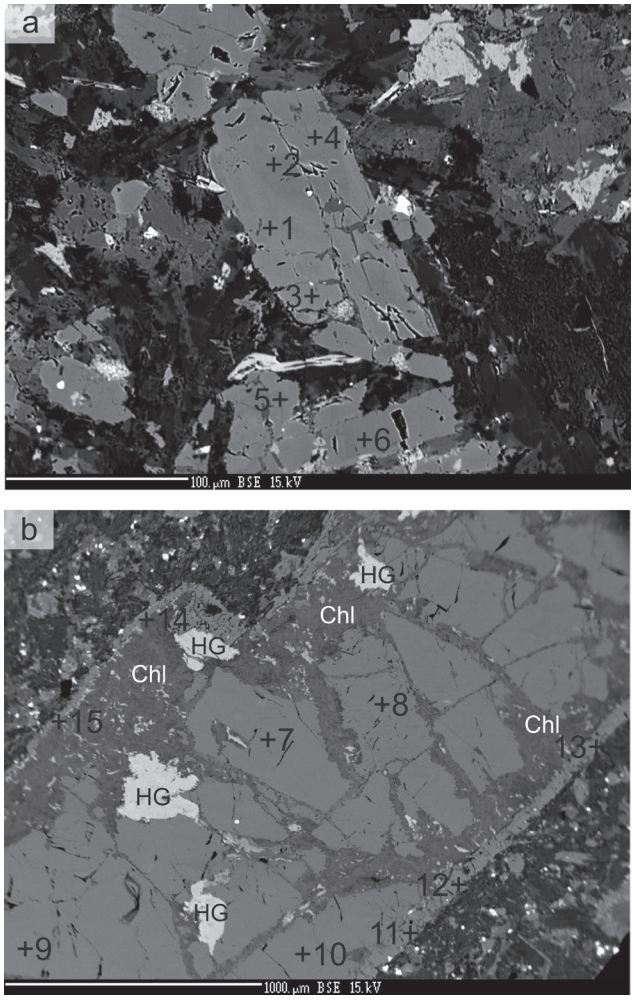

Fig. 4. a,b — Back scattered electron (BSE) images of clinopyroxenes; HG — hydrated garnet, Chl — chlorite; the numbers in figures correspond to those in Table 3.

can be classified as diopside to Ca-rich augite (Fig. 5). There are also rare occurrences of clinopyroxene xenocrysts in these rocks (Fig. 4b). They are partially altered to form a mixture of chlorite and hydrated grossular-andradite garnet. This alteration must have taken place at the lamprophyres magma generating site, as the rims of the xenocrysts were formed later. Compared to the phenocrysts, the xenocrysts have increased contents of Al_2O_3, Na_2O and TiO_2 and lower contents of SiO_2 and CaO (Table 3). The newly formed rims of xenocrysts have a similar composition to the central part of phenocrysts. An identical type of clinopyroxenes alteration was also described in the Nízke Tatry Mountains Permian basalts (Spišiak et al. 2017).

Amphibole is a relatively rare mineral (Fig. 6a) and is often strongly altered. It usually has elevated contents of TiO_2, Na_2O and K_2O (Table 4). Based on the classification of amphiboles (Hawthorne et al. 2012), it corresponds to kaersutitic amphibole based on the Ti>0.5 *apfu*. However, unknown Fe^{2+}/Fe^{3+} and $(OH)^-/O^{2-}$ ratio prevents exact classification. The Al content is too low for kaersutite. If a part of Fe is treated as trivalent to charge balance octahedral sites, amphibole would have the composition of ferri-kaersutite. In contrast, if the charge at octahedral sites is balanced by OH, the composition would be between ferro-ferri-kaersutite and hastingsite. Like amphibole, biotite is also strongly altered (chloritized). It is characterized by the high content of TiO_2, which documents its magmatic origin (Table 4). Based on the mica classification of Rieder et al. (1998), it corresponds to annite (Fig. 7). Abdel-Rahman (1993) used the dependence of Al_2O_3 and MgO in biotites from different lamprophyre types for their genetic classification. In the discrimination diagram (Fig. 8), the biotites from the rocks under study are lying in the field of biotites from calc–alkaline lamprophyres.

Plagioclase and K-feldspar are common felsic minerals in these rocks, with plagioclase prevailing over alkaline feldspar. Plagioclase has a relatively high basicity — An_{61} (Table 5, Fig. 6b). Strongly resorbed xenoliths of the surrounding granitoid rocks, and/or feldspar rarely occur. In plagioclase xenocrysts, the original composition is often preserved only in

Table 3: Selected analyses of clinopyroxenes. Crystal-chemical formula calculated based on 6 cations and Fe^{2+}/Fe^{3+} ratio calculated from charge-balanced formula. pr — prismatic sector, py — pyramidal sector, c — core, xe — xenocryst, r — rims.

N. anal.	1	2	3	4	5	6	7	8	9	10	11	12	13	14	15
Sector	pr	py	pr	py	c	c	xe	xe	xe	xe	r	r	r	r	r
SiO_2	46.33	49.96	48.29	50.04	50.27	50.36	47.03	47.29	47.04	47.06	49.18	47.96	48.70	49.29	50.77
TiO_2	2.97	1.67	2.28	1.60	1.41	1.45	1.82	1.83	1.83	1.86	1.89	2.26	1.99	1.95	1.52
Al_2O_3	6.41	2.81	4.44	2.84	3.15	2.78	8.34	8.40	8.53	8.62	4.02	4.73	3.73	4.19	2.98
Cr_2O_3	0.29	0.01	0.00	0.00	0.31	0.27	0.02	0.01	0.04	0.03	0.04	0.14	0.04	0.07	0.08
Fe_2O_3	3.34	2.10	2.74	2.91	1.92	1.41	3.21	3.02	2.42	2.77	2.49	4.30	3.05	2.45	1.81
FeO	5.47	7.16	7.18	6.36	6.49	6.69	5.62	5.93	6.41	6.17	6.17	4.79	6.19	6.53	6.86
MnO	0.17	0.27	0.31	0.25	0.26	0.24	0.20	0.22	0.23	0.18	0.21	0.22	0.19	0.28	0.23
MgO	12.40	13.83	12.35	14.15	14.79	14.65	12.92	12.90	12.71	12.87	13.27	13.33	13.28	13.42	14.22
CaO	21.57	21.37	21.58	21.24	20.78	20.97	19.26	19.28	19.17	19.06	21.89	21.77	21.64	21.36	21.61
Na_2O	0.56	0.37	0.55	0.46	0.34	0.34	0.91	0.93	0.85	0.90	0.51	0.56	0.47	0.54	0.40
K_2O	0.03	0.02	0.03	0.03	0.02	0.01	0.04	0.01	0.03	0.02	0.02	0.04	0.02	0.03	0.03
Total	99.55	99.57	99.74	99.88	99.74	99.17	99.37	99.82	99.26	99.54	99.69	100.10	99.31	100.11	100.51
Si^{4+}	1.743	1.875	1.819	1.869	1.873	1.886	1.754	1.756	1.758	1.752	1.841	1.791	1.835	1.838	1.881
Al^{3+}	0.257	0.124	0.181	0.125	0.127	0.114	0.246	0.244	0.242	0.248	0.159	0.208	0.165	0.162	0.119
Σ	2.000	1.999	2.000	1.994	2.000	2.000	2.000	2.000	2.000	2.000	2.000	1.999	2.000	2.000	2.000
Ti^{4+}	0.084	0.047	0.065	0.045	0.040	0.041	0.051	0.051	0.051	0.052	0.053	0.063	0.056	0.055	0.042
Al^{3+}	0.028	0.000	0.016	0.000	0.011	0.009	0.121	0.124	0.133	0.131	0.019	0.000	0.000	0.022	0.011
Fe^{3+}	0.095	0.059	0.078	0.082	0.054	0.040	0.090	0.084	0.068	0.078	0.070	0.121	0.087	0.069	0.050
Cr^{3+}	0.009	0.000	0.000	0.000	0.009	0.008	0.001	0.000	0.001	0.001	0.001	0.004	0.001	0.002	0.002
Mg^{2+}	0.696	0.774	0.693	0.788	0.821	0.818	0.718	0.714	0.708	0.714	0.741	0.742	0.746	0.746	0.785
Fe^{2+}	0.090	0.120	0.148	0.085	0.065	0.084	0.019	0.026	0.038	0.024	0.116	0.069	0.110	0.106	0.108
Σ	1.000	1.000	1.000	1.000	1.000	1.000	1.000	1.000	1.000	1.000	1.000	1.000	1.000	1.000	1.000
Fe^{2+}	0.083	0.105	0.078	0.113	0.137	0.126	0.156	0.158	0.162	0.168	0.077	0.080	0.085	0.097	0.105
Mn^{2+}	0.005	0.009	0.010	0.008	0.008	0.008	0.006	0.007	0.007	0.006	0.007	0.007	0.006	0.009	0.007
Ca^{2+}	0.870	0.859	0.871	0.850	0.829	0.842	0.770	0.767	0.767	0.760	0.878	0.871	0.873	0.853	0.858
Na^{+}	0.041	0.027	0.040	0.033	0.025	0.025	0.066	0.067	0.062	0.065	0.037	0.041	0.034	0.039	0.029
K^{+}	0.001	0.001	0.001	0.001	0.001	0.000	0.002	0.000	0.001	0.001	0.001	0.002	0.001	0.001	0.001
Σ	1.000	1.001	1.000	1.006	1.000	1.000	1.000	1.000	1.000	1.000	1.000	1.001	1.000	1.000	1.000
Wo	38.32 %	40.92 %	40.32 %	40.46 %	38.98 %	40.08 %	32.03 %	31.94 %	32.05 %	31.44 %	40.97 %	39.40 %	40.60 %	39.67 %	40.84 %
En	38.24 %	40.48 %	37.07 %	41.40 %	43.18 %	42.64 %	40.02 %	39.69 %	39.35 %	39.76 %	39.27 %	40.25 %	39.61 %	39.66 %	41.05 %
Fs	9.46 %	11.76 %	12.08 %	10.44 %	10.63 %	10.92 %	9.77 %	10.24 %	11.14 %	10.69 %	10.24 %	8.11 %	10.36 %	10.82 %	11.11 %
Ae	1.12 %	0.91 %	1.21 %	1.38 %	0.72 %	0.63 %	1.45 %	1.39 %	1.05 %	1.23 %	1.11 %	1.62 %	1.25 %	1.13 %	0.84 %
Jd	3.37 %	1.91 %	3.08 %	2.12 %	1.86 %	1.94 %	5.89 %	6.05 %	5.80 %	6.00 %	2.81 %	2.78 %	2.39 %	3.02 %	2.16 %
Ca–Ts	4.87 %	1.57 %	2.78 %	1.84 %	2.54 %	1.66 %	8.01 %	7.86 %	7.75 %	7.98 %	2.77 %	4.40 %	2.80 %	2.79 %	1.78 %
Ti–Ts	4.62 %	2.47 %	3.45 %	2.36 %	2.08 %	2.13 %	2.84 %	2.84 %	2.86 %	2.90 %	2.82 %	3.44 %	3.00 %	2.91 %	2.21 %

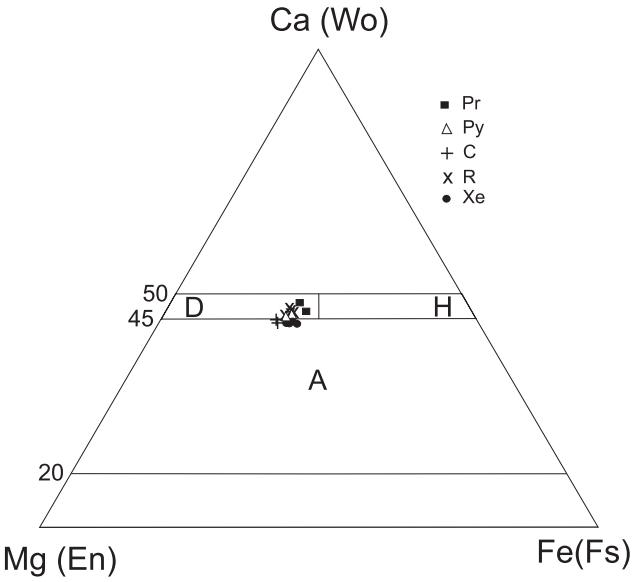

Fig. 5. Classification diagram of clinopyroxenes (Morimoto et al. 1988); D — diopside, H — hedenbergite, A — augite; pr — prismatic sector, py — pyramidal sector, c — core, r — rims, xe — xenocryst.

the central parts (basicity corresponds to the original granitoid plagioclase; An_{32} (Broska et al. 1997, Fig. 6b) and the rims are replaced by more basic plagioclase. The rims ($An_{58–61}$) of the xenoliths correspond to primary plagioclase from lamprophyres (Fig. 9). K-feldspar is less common and has elevated contents of Na_2O and Ba (Table 5).

From the accessory minerals, apatite is the most common. It forms columnar grains, or grains with a hexagonal shape (Fig. 10a). Needle-like apatite (Fig. 6a) as well as oval-shape apatite are observed in rare cases (Fig. 10b). According to their composition (Fig. 10c,d; Table 6), the apatite studied here belongs to the apatite group (Pasero et al. 2010) with the composition of hydroxylapatite. It has a low proportion of substituting cations (Fe<0.04 *apfu*, Mg<0.02 apfu, Na<0.03 *apfu*,

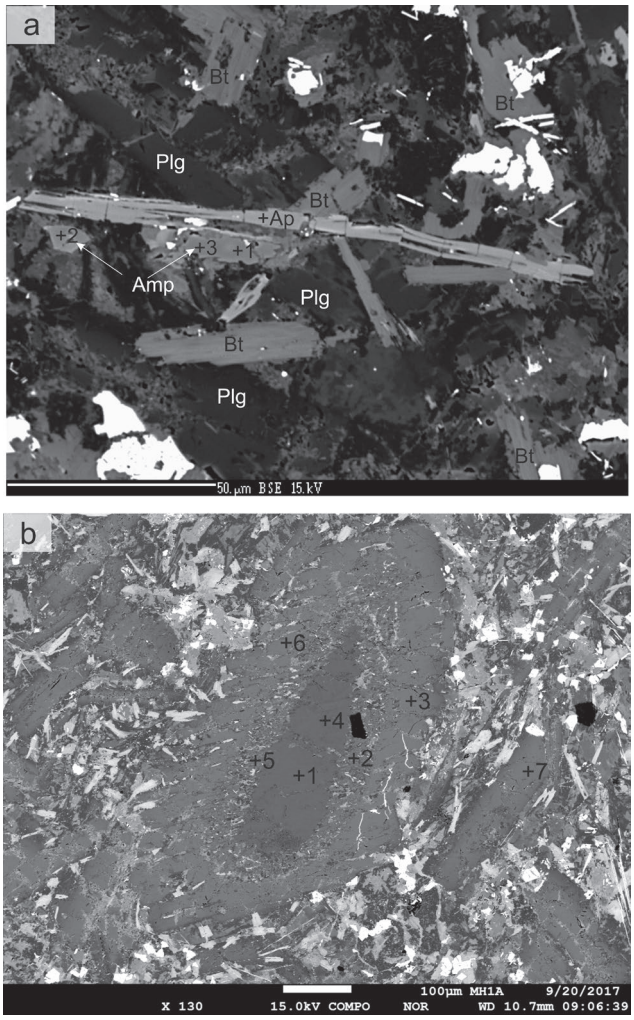

Fig. 6. a — Back scattered electron (BSE) images of amphiboles and apatites, the numbers in figures correspond to those in Table 4; **b** — back scattered electron (BSE) images of plagioclases, the numbers in figures correspond to those in Table 5; Plg — plagioclases, Amp — amphiboles, Bt — biotites, Ap — apatites.

Table 4: Selected analyses of amphiboles and biotites. Crystal-chemical formula calculated based on 13 *C+T* cations (amphiboles) and 22 negative charges (biotites).

N. anal.	1	2	3	N. anal.	1	2	3
SiO_2	39.63	40.47	39.61	SiO_2	35.35	35.03	35.29
TiO_2	5.45	4.33	5.10	TiO_2	3.58	5.47	5.92
Al_2O_3	11.23	10.41	11.22	Al_2O_3	16.24	14.53	14.66
Cr_2O_3	0.01	0.12	0.00	Cr_2O_3	0.00	0.00	0.00
FeO	16.72	20.16	16.64	FeO	23.59	22.55	21.99
MnO	0.30	0.44	0.30	MnO	0.05	0.08	0.07
MgO	8.89	7.19	8.54	MgO	8.35	8.99	9.32
CaO	11.13	11.08	11.33	CaO	0.06	0.10	0.05
Na_2O	2.45	2.65	2.29	Na_2O	0.14	0.09	0.11
K_2O	1.42	1.55	1.51	K_2O	9.34	9.46	9.48
H_2O*	1.69	1.68	1.67	H_2O*	3.90	3.89	3.92
Total	98.92	100.08	98.21	Total	100.60	100.19	100.81
Si^{4+}	6.100	6.260	6.162	Si^{4+}	2.716	2.703	2.697
Al^{3+}	1.900	1.740	1.838	$^{IV}Al^{3+}$	1.284	1.297	1.303
$\sum T$	8.000	8.000	8.000	$\sum T$	4.000	4.000	4.000
Ti^{4+}	0.631	0.504	0.597	Ti^{4+}	0.207	0.318	0.340
Al^{3+}	0.137	0.158	0.219	$^{VI}Al^{3+}$	0.187	0.025	0.017
Cr^{3+}	0.001	0.015	0.000	Cr^{3+}	0.000	0.000	0.000
Mg^{2+}	2.040	1.658	1.980	Fe^{2+}	1.516	1.455	1.405
Mn^{2+}	0.039	0.058	0.040	Mn^{2+}	0.003	0.005	0.005
Fe^{2+}	2.152	2.608	2.165	Mg^{2+}	0.956	1.034	1.062
$\sum C$	5.000	5.000	5.000	$^{M}\square$	0.131	0.162	0.171
Ca^{2+}	1.835	1.836	1.888	$\sum M$	3.000	3.000	3.000
Na^{+}	0.165	0.164	0.112	Ca^{2+}	0.005	0.008	0.004
$\sum B$	2.000	2.000	2.000	Na^{+}	0.021	0.013	0.016
Na^{+}	0.567	0.631	0.579	K^{+}	0.915	0.931	0.924
K^{+}	0.279	0.306	0.300	$^{I}\square$	0.059	0.047	0.055
$\sum A$	0.845	0.937	0.879	$\sum I$	0.941	0.953	0.945
OH^{-}	2.000	2.000	2.000	OH^{-}	2.000	2.000	2.000

REE<0.03 *apfu*) but $(OH)^-$ is significantly substituted by F^- (0.37–0.44 *apfu*) and Cl^- (0.05 *apfu*).. From the opaque minerals, the most common are ilmenite, rutile, pyrite, chalcopyrite, pyrrhotite, while the sulphides are younger than the oxides.

Discussion

Geochemical characterization of the lamprophyres

The chemical composition of the lamprophyres from the Malá Fatra Mts. can be used to reveal their genetic conditions, although it is strongly affected by the alteration of these rocks and amygdales and xenoliths of the surrounding granitoid rocks (or plagioclases) presence. In the classification diagram of different types of lamprophyre rocks (Rock 1987), the studied lamprophyres correspond to the calc–alkaline type (Fig. 11). To compare, we plotted the average compositions of calc–alkaline lamprophyres, spessartites (Rock 1991) and Cretaceous alkaline lamprophyres from the Malá Fatra Mts. (Spišiak & Hovorka 1997). The Cretaceous lamprophyres from the Malá Fatra Mts. fall within the field of alkaline lamprophyres.

For a more detailed geochemical characterization, we used a trace element diagram normalized to primitive mantle (Fig. 12). The contents of compatible elements (Cr, Ni, Co, V, Sc) in the studied lamprophyres are lower (Cr, Ni) or similar to primitive mantle (PM). This could mean that the source was either depleted in these elements or retained by compatible elements during partial melting. It could also indicate (especially Sc and Co concentrations) the presence of biotite and clinopyroxene in the source. In contrast to PM, all incompatible elements are highly abundant. Compared to the average composition of calc–alkaline lamprophyres, the lamprophyres from the Malá Fatra Mts. are rich in Nb and Ta and slightly depleted in LILE (large-ion lithophile elements), namely Rb, Ba and Cs. The other elements compared had identical contents. Enrichment of some lamprophyre types with Nb and Ta was also described in the Sudetes (Awdankiewicz 2007)

We also used discrimination diagrams to classify the studied rocks with different types of magmatic formations. The Nb/Y ratio was used as an index to ascertain the alkaline or

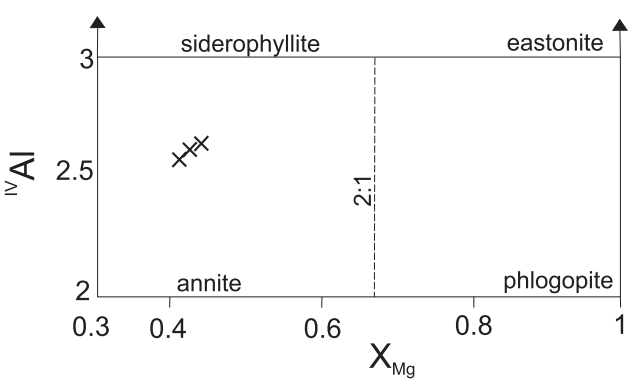

Fig. 7. Classification diagram of studied micas. End-members names according to Rieder et al. (1998).

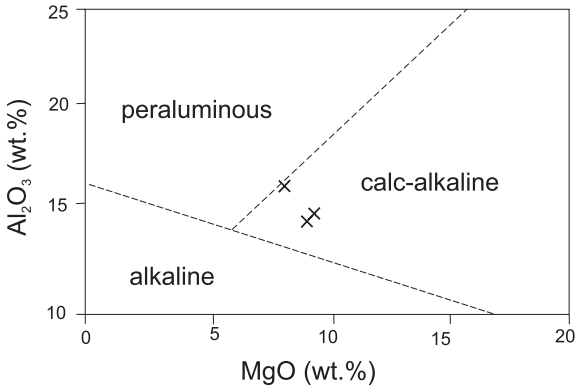

Fig. 8. Position of studied mica in the classification diagram of Abdel-Rahman (1993) for micas from different magmatic series.

Table 5: Selected analyses of plagioclases and K-feldspar.

Sample	MH-1							DS-29				DS-55	
N. anal.	1xe	2	3	4xe	5	6	7	8	9	10	11	12	13
SiO_2	59.96	55.83	52.76	60.01	54.89	52.19	52.58	53.26	53.74	53.09	53.95	64.73	65.06
TiO_2	0.00	0.14	0.21	0.11	0.10	0.08	0.10	0.00	0.00	0.00	0.00	0.00	0.00
Al_2O_3	25.15	27.61	29.45	25.08	28.19	29.74	29.74	28.54	28.40	29.04	28.56	18.36	18.08
FeO	0.24	0.41	0.43	0.22	0.32	0.42	0.38	0.49	0.43	0.53	0.55	0.20	0.17
MnO	0.00	0.09	0.03	0.00	0.00	0.07	0.03	0.00	0.00	0.00	0.00	0.00	0.01
CaO	6.21	9.38	11.92	6.27	9.99	12.36	12.07	12.44	12.29	12.57	11.38	0.09	0.05
MgO	0.00	0.06	0.05	0.00	0.02	0.05	0.03	0.08	0.09	0.11	0.11	0.23	0.00
BaO	0.06	0.03	0.04	0.04	0.04	0.12	0.04	0.00	0.00	0.00	0.00	0.34	0.17
SrO	0.26	0.23	0.25	0.36	0.25	0.16	0.12	0.13	0.15	0.13	0.16	0.00	0.00
Na_2O	7.52	5.49	4.28	7.17	5.03	4.02	4.17	3.94	4.32	3.99	4.52	0.47	0.45
K_2O	0.91	0.87	0.42	0.89	0.85	0.36	0.39	0.59	0.53	0.43	0.75	15.91	16.27
Total	100.30	100.14	99.83	100.15	99.69	99.55	99.64	99.48	99.95	99.90	99.98	100.33	100.26
Formula based on 5 cations													
Si	2.67	2.52	2.40	2.69	2.49	2.39	2.40	2.44	2.44	2.42	2.45	2.99	3.00
Ti	0.00	0.00	0.01	0.00	0.00	0.00	0.00	0.00	0.00	0.00	0.00	0.00	0.00
Al	1.32	1.47	1.58	1.32	1.51	1.60	1.60	1.54	1.52	1.56	1.53	1.00	0.98
Cr	0.00	0.00	0.00	0.00	0.00	0.00	0.00	0.00	0.00	0.00	0.00	0.00	0.00
Fe3	0.00	0.00	0.00	0.00	0.00	0.00	0.00	0.00	0.00	0.00	0.00	0.00	0.00
Fe2	0.01	0.02	0.02	0.01	0.01	0.02	0.01	0.02	0.02	0.02	0.02	0.01	0.01
Mn	0.00	0.00	0.00	0.00	0.00	0.00	0.00	0.00	0.00	0.00	0.00	0.00	0.00
Mg	0.00	0.00	0.00	0.00	0.00	0.00	0.00	0.01	0.01	0.01	0.01	0.02	0.00
Ca	0.30	0.45	0.58	0.30	0.49	0.61	0.59	0.61	0.60	0.61	0.55	0.00	0.00
Ba	0.00	0.00	0.00	0.00	0.00	0.00	0.00	0.00	0.00	0.00	0.00	0.01	0.00
Na	0.65	0.48	0.38	0.62	0.44	0.36	0.37	0.35	0.38	0.35	0.40	0.04	0.04
K	0.05	0.05	0.02	0.05	0.05	0.02	0.02	0.03	0.03	0.03	0.04	0.94	0.96
An	29.69	46.09	59.11	30.85	49.70	61.60	60.11	61.36	59.25	61.87	55.63	0.47	0.26
Ab	65.11	48.84	38.43	63.92	45.28	36.27	37.55	35.17	37.70	35.59	39.97	4.23	4.03
Or	5.20	5.06	2.46	5.23	5.02	2.14	2.34	3.46	3.05	2.54	4.39	95.30	95.71

calc–alkaline character of various rock types (Ma et al. 2013, Jayabalan et al. 2015). The high Nb contents in the samples would point to their alkaline character. A similar dependence was used by Krmíček et al. (2011) for geotectonic classification. In the discrimination diagram (Fig. 13), the examined rocks are lying in the field of anorogenic geodynamic setting rocks. Further, we employed the dependence of Th/Y; Ta/Yb and Ba/Th, U/La to compare the studied lamprophyres with main geochemical reservoirs (Fig. 14a,b). In the diagrams, the rocks lie close to the enriched mantle field (Fig. 14a) or are shifted toward U–Th enrichment (Fig. 14b). We also plotted the analyses of calc–alkaline lamprophyres from the Krušné hory Mts. (Štemprok et al. 2014).

The normalized REE curve (Fig. 15) indicates enrichment in LREE relative to HREE, which can result from moderate-degrees of partial melting of the protolith. No Eu-anomaly was observed and therefore, no accumulation or plagioclase fractionation during magma evolution is likely. La/Yb ratio from the sampled lamprophyres is consistently within 0.14 to 0.17 indicating that parental melts were probably mantle-derived

(Sun & McDonough 1989). In comparison to the REE curve, in calc–alkaline lamprophyres, lower LREE and slightly higher HREE contents can be observed.

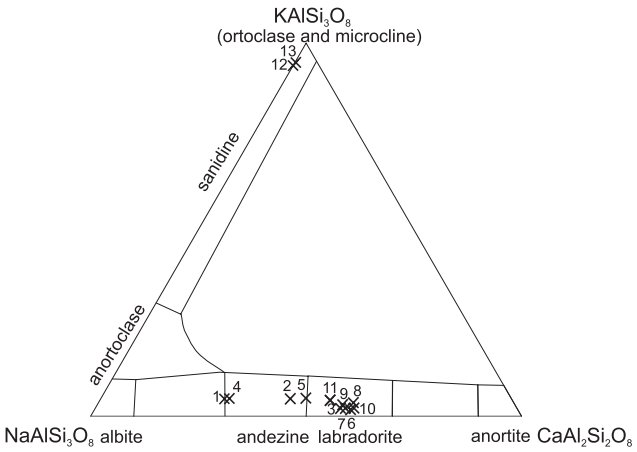

Fig. 9. Classification diagram of feldspars; the numbers in figures correspond to those in Table 5.

The available data on Sr and Nd isotopes indicate relatively large differences in the composition (Bernard-Griffiths et al. 1991; Rock 1991; Huang et al. 1998; Seifert 2009 and others) of different varieties of calc–alkaline lamprophyre. Relatively large variations in the chemical composition of these rocks (including Sr and Nd isotopic compositions) are probably a result of primary magma contamination by crustal material during magma ascent. Our isotopic data (Table 2; Fig. 16) suggest that the mantle was the primary source of magma (ε_{Nd}=4), but it was affected by crustal material. Similar isotope contents are found in some lamprophyre types from the Mid-European Variscides (Seifert 2009).

The genetical remarks to lamprophyres

The Late Paleozoic lamprophyres of the Malá Fatra Mts. have a complicated genesis influenced by contamination of primary magma with mantle material. Geochemistry and mineralogy indicate their calk–alkaline to alkaline character. The mineral association including diopside, biotite and plagioclase is typical for calc–alkaline lamprophyres (Rock 1987).

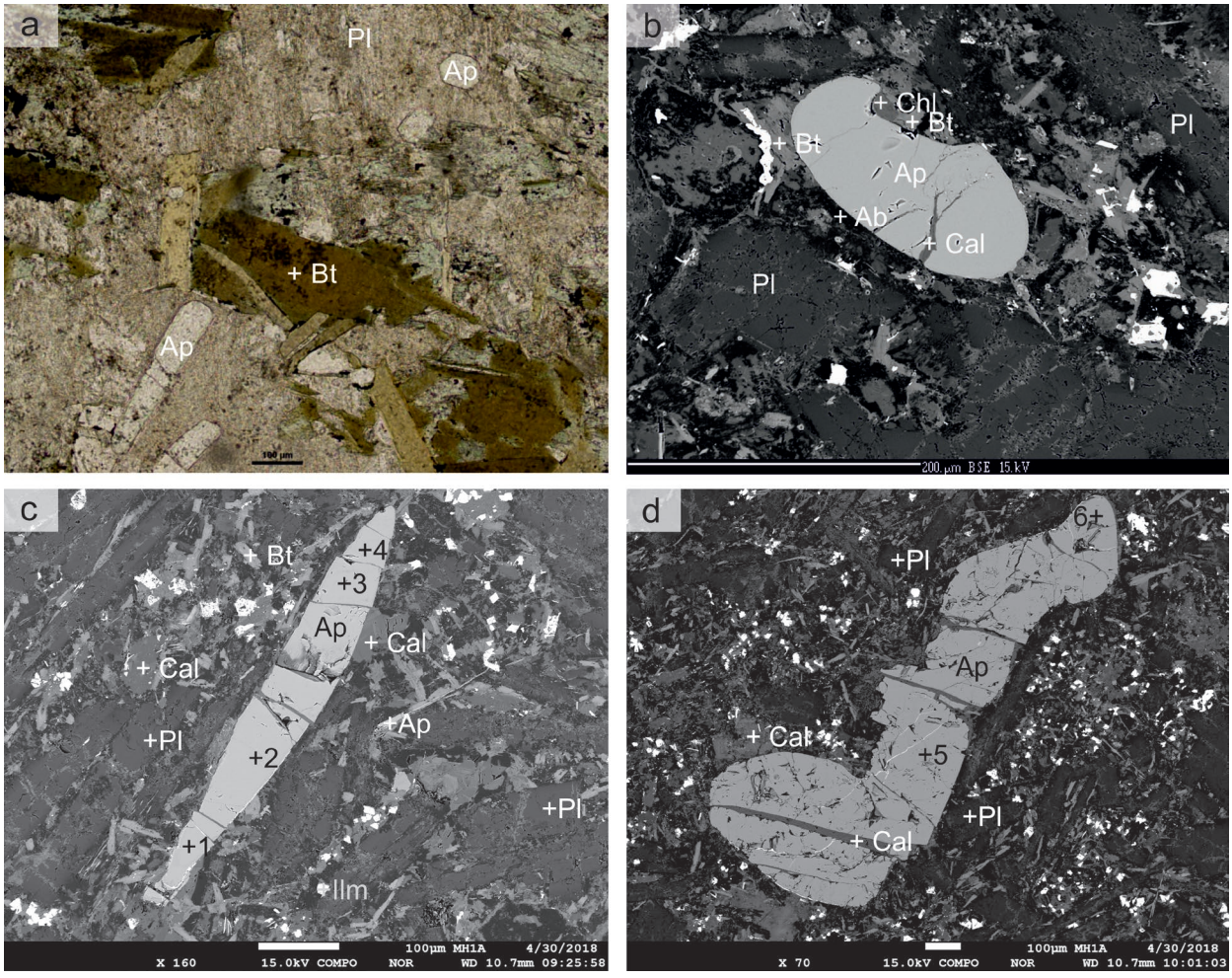

Fig. 10. a — Photomicrograph of lamprophyres, parallel polaroids; **b,c,d** — back scattered electron (BSE) images of apatite in studied lamprophyres; the numbers in figures correspond to those in Table 6; Pl — plagioclases, Bt — biotites, Ap — apatites, Chl — chlotites, Ab — albite, Cal — calcite, Ilm — ilmenite.

Table 6: Selected analyses of apatites.

N. anal.	1	2	3	4	5	6
Figures	Fig 10c				Fig. 10d	
SiO_2	0.13	0.14	0.15	0.15	0.10	0.09
TiO_2	0.00	0.00	0.00	0.08	0.09	0.05
Al_2O_3	0.00	0.00	0.00	0.03	0.00	0.00
FeO	0.55	0.47	0.54	0.51	0.53	0.58
MnO	0.11	0.20	0.14	0.16	0.16	0.12
MgO	0.10	0.10	0.10	0.11	0.14	0.17
CaO	52.79	52.51	52.85	52.81	52.27	52.70
Na_2O	0.14	0.11	0.13	0.09	0.10	0.10
K_2O	0.01	0.01	0.00	0.02	0.01	0.00
BaO	0.07	0.05	0.01	0.00	0.00	0.00
F	1.53	1.36	1.49	1.41	1.53	1.63
Cl	0.35	0.36	0.35	0.34	0.34	0.34
SrO	0.10	0.09	0.09	0.12	0.12	0.10
SO_3	0.00	0.00	0.01	0.00	0.02	0.01
ThO_2	0.02	0.03	0.00	0.01	0.02	0.00
PbO	0.04	0.00	0.00	0.00	0.02	0.02
P_2O_5	41.14	41.43	41.69	41.36	41.48	41.47
Y_2O_3	0.08	0.02	0.08	0.04	0.03	0.02
La_2O_3	0.13	0.18	0.13	0.17	0.10	0.11
Ce_2O_3	0.33	0.40	0.33	0.36	0.26	0.25
Pr_2O_3	0.01	0.07	0.01	0.01	0.10	0.00
Nd_2O_3	0.16	0.15	0.14	0.16	0.15	0.13
Sm_2O_3	0.02	0.00	0.03	0.06	0.01	0.00
Total	97.78	97.66	98.26	98.00	97.58	97.89
Oxygens	13	13	13	13	13	13
P	3.005	3.030	3.023	3.015	3.024	3.012
Si	0.011	0.012	0.013	0.013	0.009	0.008
S	0.000	0.000	0.000	0.000	0.001	0.001
sum	3.016	3.042	3.036	3.028	3.034	3.021
Ca	4.880	4.861	4.850	4.872	4.823	4.845
Al	0.000	0.000	0.000	0.003	0.000	0.000
Ti	0.000	0.000	0.000	0.005	0.006	0.003
Fe	0.039	0.034	0.039	0.037	0.038	0.041
Mn	0.008	0.014	0.010	0.012	0.012	0.008
Mg	0.013	0.012	0.013	0.014	0.018	0.021
Na	0.023	0.018	0.022	0.016	0.017	0.017
K	0.001	0.001	0.000	0.003	0.001	0.000
Ba	0.002	0.002	0.000	0.000	0.000	0.000
Sr	0.005	0.005	0.004	0.006	0.006	0.005
Th	0.000	0.001	0.000	0.000	0.000	0.000
Pb	0.001	0.000	0.000	0.000	0.001	0.001
REE+Y	0.024	0.026	0.023	0.025	0.021	0.016
sum	4.995	4.973	4.962	4.992	4.942	4.958
F	0.418	0.372	0.402	0.385	0.417	0.442
Cl	0.051	0.052	0.051	0.050	0.050	0.049
OH	0.531	0.576	0.547	0.565	0.533	0.509
sum F+Cl	0.469	0.424	0.453	0.435	0.467	0.491
Y	0.004	0.001	0.004	0.002	0.001	0.001
La	0.004	0.006	0.004	0.005	0.003	0.003
Ce	0.010	0.013	0.010	0.011	0.008	0.008
Pr	0.000	0.002	0.000	0.000	0.003	0.000
Nd	0.005	0.005	0.004	0.005	0.005	0.004
Sm	0.000	0.000	0.001	0.002	0.000	0.000
Total	14.511	14.450	14.450	14.485	14.418	14.453

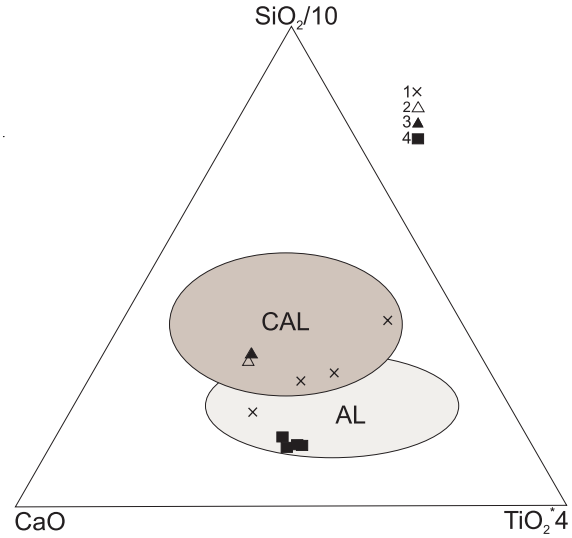

Fig. 11. Classification diagram of lamprophyres (Rock 1987); 1 — studied lamprophyres, 2 — calc–alkaline lamprophyres, 3 — average spessartite (data for calc–alkaline lamprophyres and spessartite from Rock (1991), 4 — Cretaceous alkaline lamprophyres from Malá Fatra Mts. (Hovorka & Spišiak 1988).

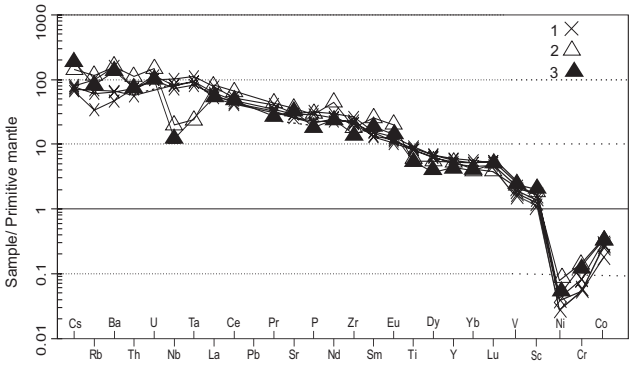

Fig. 12. Trace element concentrations normalized to the composition of the primordial mantle (McDonough & Sun 1995); 1— studied lamprophyres, 2 — calc–alkaline lamprophyres, 3 — average spessartite (data for calc–alkaline lamprophyres and spessartite from Rock (1991).

However, the Ti enrichment in pyroxene and biotite, presence of kaersutitic amphibole indicates an alkaline trend (Rock 1987), although similar magmatic kaersutite was reported from calc–alkaline lamprophyres (Pivec et al. 2002). Apatite in the studied samples has a relatively lower F content compared to typical apatite from lamprophyres (e.g., Tappe et al. 2006; Seifert 2009; Pandey et al. 2018) or magmatic apatite from granitic rocks in the Western Carpathians (Broska et al. 2004). In contrast, the Cl content in apatite is unusually high compared to granitoids in the Western Carpathians (Broska et al. 2004) and most of lamprophyres (e.g., Renno et al. 2003; Tappe et al. 2006; Pandey et al. 2018). However, high Cl content in apatite is typical for post-collisional lamprophyres (Seifert 2009).

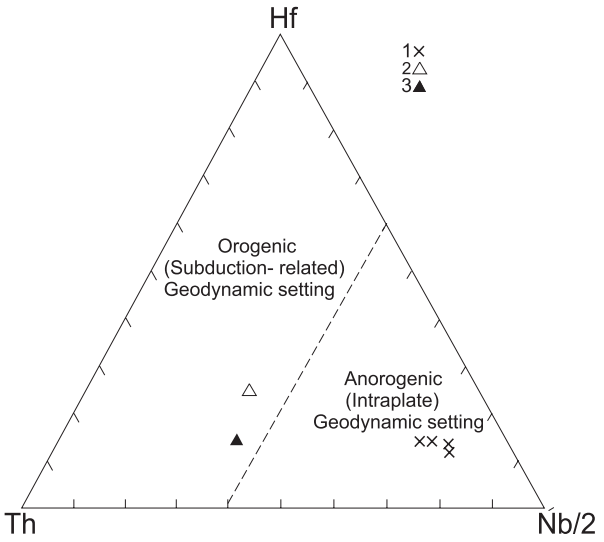

Fig. 13. Discriminant diagram Th–Hf–Nb/2 for orogenic and anorogenic lamproites (Krmíček et al. 2011); 1— studied lamprophyres, 2 — calc–alkaline lamprophyres, 3 — average spessartite (data for calc–alkaline lamprophyres and spessartite from Rock (1991).

It is assumed that primary magma was derived from enriched mantle protolith influenced by crustal contamination by sediments and assimilation of surrounding granitoid rocks. In comparison with similar calc–alkaline Late Paleozoic lamprophyres from other Western Carpathians localities, such as the Low Tatras, they are different in the content of individual minerals (especially amphibole) as well as overall geochemistry. If compared with Malá Fatra Cretaceous alkaline lamprophyres (Polom, Višňové or Krpeľany), Malá Fatra Late Paleozoic lamprophyres have a different geological position (cut carbonate sequences of Krížna nappe), different age, moderately different mineral and chemical composition, they contain foids and lack quartz and feldspar. At the same time, the alkaline type of rocks has not been reported from the Western Carpathians Late Paleozoic.

The studied lamprophyres contain clinopyroxene (Cpx) xenocrysts partially altered to a mixture of hydrated garnets and chlorite. Cpx xenocrysts are fringed with newly formed Cpx identical in content with porphyric xenocrysts. An identical type of alteration of clinopyroxenes was also described in the case of clinopyroxenes from Nízke Tatry Permian basalts (Spišiak et al. 2017). The hydrated garnets and chlorites in

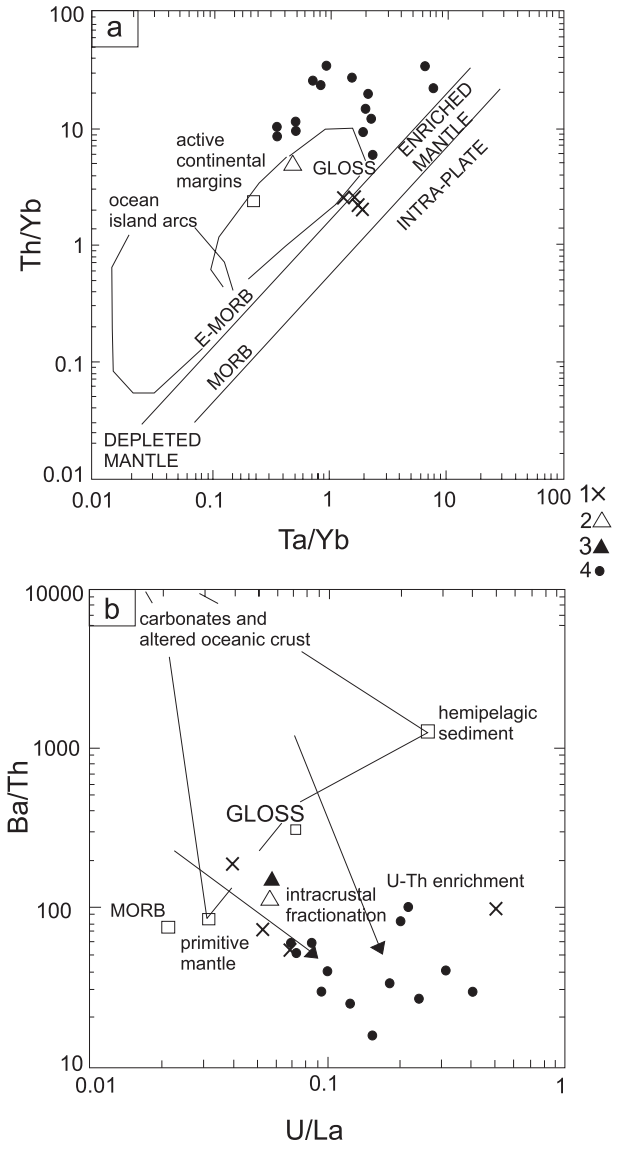

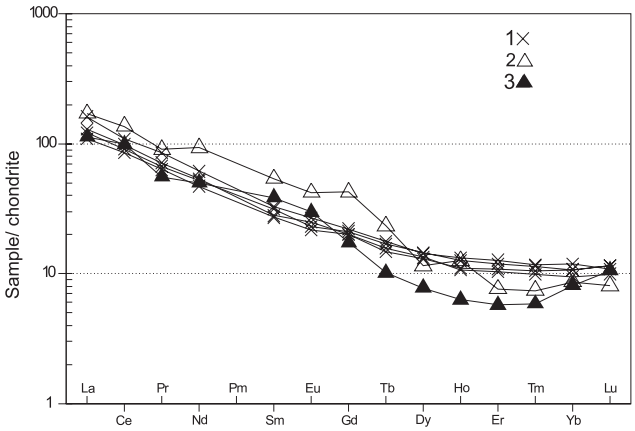

Fig. 15. Chondrite (McDonough & Sun 1995) normalized diagram; 1 — studied lamprophyres, 2 — calc–alkaline lamprophyres, 3 — average spessartite (data for calc–alkaline lamprophyres and spessartite from Rock (1991).

Fig. 14. Trace element variation diagram for studied lamprophyres and the main geochemical reservoirs; **a** — Th/Yb:Ta/Yb (Wilson 1989; Pearce 1993); **b** — Ba/Th:U/La (Patino et al. 2000); GLOSS — global oceanic subducting sediment (Plank & Langmuir 1998); 1 — studied lamprophyres, 2 — calc–alkaline lamprophyres, 3 — average spessartite (data for calc–alkaline lamprophyres and spessartite from Rock (1991), 4 — Krušné Hory Mts. lamprophyres (data from Štemprok et al. 2014).

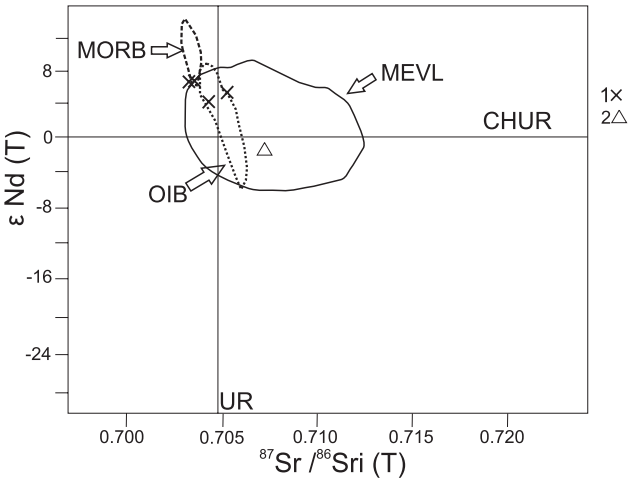

Fig. 16. Initial Nd–Sr rations of studied lapmprophyres in comparison with different mantle rocks; 1 — studied lamprophyres, 2 — average calc–alkaline lamprophyres (Rock 1991), MORB — Mid-Ocen Ridge Basalts, OIB — Ocean Island Basalts (Faure 1986), MEVL — Mid-European Variscides Lamprophyres (Seifert 2009), CHUR — Chondrit Uniform Reservoir, UR — Undifferent Reservoir (DePaolo & Wasserburg 1976).

both types of rocks are very similar in composition. Regarding the fact they are xenocrysts, we suppose that they grew in the basic melt at great depth, at the site of its generation. The same age of rocks, the same type of xenocrysts and the same type of their alteration point to possible comagmatic origin of Permian paleobasalts (melaphyres) in the Hronicum and Late Paleozoic calc–alkaline lamprophyres from the Malá Fatra Mountains.

The age of the studied rocks has not been precisely determined yet and it is thus estimated according to their geological position. The lamprophyre dykes cut the Variscan medium-grained granodiorities to tonalities, but do not penetrate the cover Mesozoic complexes. The age of the surrounding granites was determined by Scherbak et al. (1990) at 353 Ma. In general, the age of lamprophyre is estimated to Late Paleozoic. The determined age of the rocks using LA-ICP-MS by apatite analysis of 263.4±2.6 Ma corresponds to their geological position.

Conclusions

The lamprophyric dyke rocks in the Malá Fatra core mountain which intruded the Variscan granites are strongly altered.

Xenoliths of the surrounding granite rocks and minerals (especially plagioclase) are frequently observed and they are resorbed to different degrees.

Clinopyroxene, amphibole, biotite, plagioclase and potassium feldspar are preserved as primary minerals. Clinopyroxene occurs as phenocrysts, but rarely also as xenocrysts. These two types of clinopyroxene are different in chemical composition. Amphibole (kaersutitic) and biotite are characteristic for high TiO_2 content.

Based on the main and rare element content, they correspond to calc–alkaline lamprophyres with an affinity to alkaline lamprophyres.

Variations in the chemical composition of lamprophyres (including Sr and Nd isotopic compositions) are probably the result of the primary mantle magma contamination by crustal materials.

The LA-ICP-MS U–Pb age for apatite from Malá Fatra Mts. lamprophyres is 263.4±2.6 Ma. The age is similar to the calc–alkaline lamprophyres from the Nízke Tatry Mts.

Acknowledgements: This research was supported by grants VEGA 1/0650/15, 1/0237/18 and APVV 15-0050. We appreciate the critical reviews by handling editors Pavel Uher and Igor Broska, an anonymous reviewer, and Jaromír Ulrych, who helped to improve the manuscript.

References

Abdel-Rahman A.M. 1993: Nature of biotites from alkaline, calcalkaline, and peraluminous magmas. *J. Petrol.* 35, 525–541.

Anczkiewicz R., Platt J.P., Thirwall M.F. & Wakabayashi J. 2004: Franciscan subduction off to a slow start: evidence from high-precision Lu–Hf garnet ages on high grade-block. *Earth Planet. Sci. Lett.* 225, 147–161.

Anczkiewicz R. & Thirwall M.F. 2003: Improving precision of Sm–Nd garnet dating by H_2SO_4 leaching: A simple solution to the phosphate inclusion problem. *Geol. Soc. Spec. Publ.* 220, 83–91.

Awdankiewicz M. 2007: Late Palaeozoic lamprophyres and associated mafic subvolcanic rocks of the Sudetes (SW Poland): petrology, geochemistry and petrogenesis. *Geologia Sudetica* 39, 11–97.

Bergman S.C. 1987: Lamproites and other potassium-rich igneous rocks: A review of their occurrence, mineralogy and geochemistry. In: Fitton J.G. & Uption B.G.J. (Eds.): Alkaline Igneous Rocks. *Geol. Soc. London, Spec. Publ.* 30, 103–189.

Bernard-Griffiths J., Fourcade S. & Dupuy C. 1991: Isotopic study (Sr, Nd, O and C) of lamprophyres and associated dykes from Tamazert (Morroco): crustal contamination processes and source characteristics. *Earth Planet Sci. Lett*. 103, 190–199.

Broska I., Petrík I. & Benko P. 1997: Petrology of the Malá Fatra granitoid rocks (Western Carpathians, Slovakia). *Geol. Carpath.* 48, 1, 27–47.

Broska I., Williams C.T., Uher P., Konečný P. & Leichmann J. 2004: The geochemistry of phosphorus in different granite suites of the Western Carpathians, Slovakia: the role of apatite and P-bearing feldspar. *Chem. Geol*. 205, 1–15.

Chew D.M. & Donelick R.A. 2012: Combined apatite fission track and U–Pb dating by LA-ICP MS and future trends in apatite provenance analysis. In: Sylvester P. (Ed.): Quantitative mineralogy and microanalysis of sediments and sedimentary rocks. *Mineral. Assoc. Canada*, 219–248.

Chew D.M., Petrus J.A. & Kamber B.S. 2014: U–Pb LA-ICPMS dating using accessory mineral standards with variable common Pb. *Chem. Geol*. 363C, 185–199.

Cochrane R., Spikings R.A., Chew D., Wotzlaw J.-F., Chiaradia M., Tyrrell S., Schaltegger U. & Van der Lelij R. 2014: High temperature (>350 °C) thermochronology and mechanisms of Pb loss in apatite. *Geochim. Cosmochim. Acta* 127, 39–56.

DePaolo D.J. 1981: Trace element and isotopic effects of combined wallrock assimilation and fractional crystallization. *Earth Planet. Sci. Lett*. 53, 184–202.

DePaolo D.J. & Wasserburg G.J. 1976: Inferences about magma sources and mantle structure from variations of $^{143}Nd/^{144}Nd$. *Geophys. Res. Lett.* 3, 743–746.

Faure G. 1986: Principles of Isotope Geology. *Wiley & Sons*, New York, 1–589.

Gümbel C.W. 1874: Die paläolithischen Eruptivgesteine des Fichtelgebirges. *Universitätsbuchdruckerei von J.G. Weiss*, München, 1–50.

Hawthorne C.F., Oberti R., Harlow G.E., Maresch V.W., Martin F.R., Schumacher C.J. & Welch D.M. 2012: Nomenclature of the amphibole supergroup. *Am. Mineral.* 97, 2031–2048.

Hovorka D. 1967: Porphyres and lamprophyres from tatraveporide cristalline complexes. *Sbor. geol. vied* 8, 51–78 (in Slovak).

Hovorka D. & Spišiak J. 1988: Mesozoic volcanism of the Western Carpathians. *Veda*, Bratislava, 1–263 (in Slovak).

Huang Z.L., Jin Z., Zhu Ch., Wang L. & Li X. 1998: The Sr, Nd isotopic composition of lamprophyres in Laowangzhai gold orefield, Yunnan Province. *Chin. Sci. Bull*. 43, 1, 950–954.

Ivanov M. & Kamenický I. 1957: Notes to geology and petrography Malá Fatra Mts. Cristalline. *Geol. práce* 45, 187–212 (in Slovak).

Jacobsen S.B. & Wasserburg G.J. 1980: Sm–Nd isotope evolution of chondrites. *Earth Planet. Sci. Lett.* 50, 139–155.

Jayabalan M., Udayasankar S., Thiagarajan J., Sasikumar S., Nandhakumar E., Rajakumaran M., Manikandan M. & Nagamani S. 2015: Petrology and geochemistry of lamprophyre rock types of Salem, Dharmapuri, Krishnagiri and Namakkal district, Tamil Nadu. *J. Appl. Geochem.* 17, 2, 213–235.

Kamenický L., Macek J. & Krištín J. 1987: Contribution to the petrography and geochemistry of granitoids in the Malá Fatra Mts., West Carpathians. *Mineralia Slov*aca 19, 4, 311–324 (in Slovak).

Krmíček L., Cempírek J., Havlín A., Přichystal A., Houzar S., Krmíčková M. & Gadas P. 2011: Mineralogy and petrogenesis of a Ba–Ti–Zr-rich peralkaline dyke from Šebkovice (Czech Republic): Recognition of the most lamproitic Variscan intrusion. *Lithos* 121, 74–86.

Ma L., Jiang S.Y., Hou M.L., Dai B.Z., Jiang Y.H., Yang T., Zhao K.D., Pu W., Zhu Z.Y. & Xu B. 2013: Geochemistry of Early Cretaceous calc–alkaline lamprophyres in the Jiaodong Peninsula: Implication for lithospheric evolution of the eastern North China Craton. *Gondwana Res.* 25, 2, 859–872.

McDonough W.F. & Sun S.S. 1995: Composition of the Earth. *Chem. Geol.* 120, 228.

McDowell F.W., McIntosh W.C. & Farley K.A. 2005: A precise $^{40}Ar–^{39}Ar$ reference age for the Durango apatite (U–Th)/He and fission-track dating standard. *Chem. Geol*. 214, 249–263.

McKenzie D. 1989: Some remarks on the movement of small melt fractions in the mantle. *Earth Planet. Sci. Lett.* 95, 53–72.

Morimoto N., Fabries J., Ferguson A. K., Ginzburg I.V., Ross M., Seifert F. A., Zussman J., Aoki K. & Gottardi G. 1988: Nomenclature of pyroxenes. *Am. Mineral*. 73, 1123–1133.

Pandey R., Chalapathi Rao N.V., Dhote P., Pandit D., Choudhary A.K., Sahoo S. & Lehmann B. 2018: Rift-associated ultramafic lamprophyre (damtjernite) from the middle part of the Lower Cretaceous (125 Ma) succession of Kutch, northwestern India: tectonomagmatic implications. *Geosci. Frontiers*, in press.

Pasero M., Kampf A.R., Ferraris C., Pekov I.V. Rakovan J. & White T.J. 2010: Nomenclature of the apatite supergroup minerals. *Eur. J. Mineral*. 22, 163–179.

Patino L.C., Carr M.J.& Feigenson M.D. 2000: Local and regional variations in Central American arc lavas controlled by variations in subducted sedimentary input. *Contrib. Mineral. Petrol.* 138, 265–283.

Paton C., Hellstrom J., Paul B., Woodhead J. & Hergt J. 2011: Iolite: freeware for the visualisation and processing of mass spectrometric data. *J. Anal. At. Spectrom*. 26, 2508–2518.

Pearce J.A. 1983: The role of sub-continental lithosphere in magma genesis at destructive plate margins. In: Hawkesworth C.J. & Norry M.J. (Eds.): Continental Basalts and Mantle Xenoliths. *Shiva,* Nantwich, 230–249.

Peryt T.M., Hryniv S.P. & Anczkiewicz R. 2010: Stroncium isotope composition of Badenian (Middle Miocene) Ca-sulphate deposits in West Ukraine: A preliminary study. *Geol. Quarterly* 54, 465–476.

Petrus J.A. & Kamber B.S. 2012: Vizual age: A novel approach to laser ablation ICP-MS U–Pb geochronology data reduction. *Geostand. Geoanal. Res.* 36, 3, 247–270.

Pivec E., Holub F.V., Lang M., Novák J.K. & Štemprok M. 2002: Rock-forming minerals of lamprophyres and associated mafic dykes from the Krušné hory/Erzgebirge (Czech Republic). *J. Czech. Geol. Soc*. 47, 1, 23–32.

Plank T. & Langmuir CH. 1998: The chemical composition of subducting sediment and its consequences for the crust and mantle. *Chem. Geol.* 145, 325–394.

Renno A.D., Haser S., Stanek K.P. & Götze J. 2003: Mineral Chemistry and Petrogenesis of Ultramafic Alkaline Lamprophyre Dyke from the Klunst Quarry in Ebersbach (Lusatia, Germany). *GeoLines* 15, 133–139.

Rieder M., Cavazzini G., D'Yakonov Y.S., Frank-Kamenetskii V.A., Gottardi G., Guggenheim S., Koval P.V., Müller G., Neiva A.M.R., Radoslovich E.W., Robert J.L., Sassi F.P., Takeda H., Weiss Z. & Wones D.R. 1998: Nomenclature of micas. *Canad. Mineral*. 36, 905–912.

Rock N.M.S. 1987: The nature and origin of lamprophyres an overview. In: Fitton J.G. & Upton B.G.J. (Eds): Alkaline Ingneous Rocks. *Geol.Soc. Spec. Publ*. 30, 191–226.

Rock N.M.S. 1991: Lamprophyres. *Blackie and Son Ltd*., 1–285.

Scherbak N.P., Cambel B., Bartnicky E.N. & Stenyuk L.M. 1990: U–Pb age of granitoid rock from Dubná Skala — Malá Fatra Mts. *Geol. Carpath.* 41, 407–414.

Schoene B. & Bowring S.A. 2006: U–Pb systematics of the McClure Mountain syenite: thermochronological constraints on the age of the $^{40}Ar/^{39}Ar$ standard MMhb. *Contrib. Mineral. Petrol.* 151, 5, 615–630.

Seifert W. 2005: REE–Zr and Th rich titanite and associated accessory minerals from a Kersentite in Frankenwald, Germany. *Mineral. Petrol.* 84, 129–146.

Seifert T. 2009: Metallogeny and petrogenesis of lamprophyres in the Mid-European Variscides: Post-collisional magmatism and its relationship to late-variscan ore forming processes in the Erzgebirge (Bohemian Massif). *Millpress,* Rotterdam, 1–303.

Spišiak J. 1999: Mesozoic alkali lamprophyres dyke from Polom quarry near Žilina (Malá Fatra Mts., Western Carpathians). *Mineralia Slov*aca 31, 2, 109–116 (in Slovak).

Spišiak J. & Hovorka D. 1997: Petrology of the Western Carpathians Cretaceous primitive alkaline volcanics. *Geol. Carpath.* 48, 2, 113–121.

Spišiak J. & Hovorka D. 1998: Mafic dykes in Variscan tonalities of the Malá Fatra Mts. Western Carpathians, *Slov. Geol. Mag*. 4, 3, 157–164.

Spišiak J., Vozárová A., Vozár J., Ferenc Š., Mikuš T. & Šimonová V. 2017: Fe^{3+} rich katoite from Permian basalts (Hronicum, Western Carpathians, Slovakia); composition and origin. *Carpath. J. Earth Environ. Sci.* 12, 1, 293–299.

Sun S.S. & McDonough W.F. 1989: Chemical and isotopic systematic of oceanic basalts: implications for mantle composition and processes. In: Saunders A.D. & Norry M.J. (Eds.): Magmatism in the Ocean Basins. *Geol. Soc. London, Spec. Publ.* 42, 313–345.

Štemprok M., Dolejš D. & Holub F.V. 2014: Late Variscan calc–alkaline lamprophyres in the Krupka ore district, Eastern Krušné Hory/Erzgebirge: their realtionship to Sn-W mineralization. *J. Geosci.* 59, 41–68.

Tappe S., Foley S.F., Jenner G.A., Heaman L.M., Kjarsgaard B.A., Romer R.L., Stracke A., Joyce N. & Hoefs J. 2006: Genesis of ultramafic lamprophyres and carbonatites at Aillik Bay, Labrador: a consequence of incipient lithospheric thinning beneath the North Atlantic Craton. *J. Petrol.* 47, 1261–1315.

Thomson S.N., Gehrels G.E., Ruiz J. & Buchwaldt R. 2012: Routine low-damage apatite U-Pb dating using laser ablation-multicollector-ICPMS. *Geochem. Geophys. Geosyst*. 13, 2, 23.

Ulrych J., Pivec E., Žák K., Bendl J. & Bosák P. 1993: Alkaline and ultramafic carbonate lamprophyres in Central Bohemian Carboniferous basins, Czech Republic. *Mineral. Petrol*. 48, 65–81.

Wilson M. 1989: Igneous petrogenesis. A global tectonic approach. *Chapman & Hall,* London, 1–466.